

# Multilinear Isotropic and Multilinear Kinematic Hardening on AZ31 Magnesium Alloy



Venkata Sai Prashanth Sudula

**Abstract:** Magnesium and its alloys are turning out to be increasingly more utilized in the aviation and automobile industry due to its low weight. The technology has endured numerous enhancements enabling magnesium alloys to have a mechanical performance close to aluminium alloys and prevention from corrosion. This enables numerous potential applications for magnesium alloys subjected to multiaxial fatigue. To perform the plastic deformation on AZ31 alloy, we have utilised two techniques of multilinear hardening methods. i) isotropic hardening, ii) Kinematic hardening. To come up with an accurate result, we leveraged ANSYS software to perform the simulation with accuracy and precision. on arriving to the conclusion our goal towards analysing the multilinear properties of the AZ31 alloy with two mesh size 0.4 and 0.6mm.

**Keywords:** Engineering Alloys, Mechanical Properties, Al-Mg Alloys, Az31 Mechanical Properties, Multilinear Isotropic Hardening, Multilinear Kinematic Hardening Curves, Linear Element, And Quadratic Element Type.

## I. INTRODUCTION

Aluminium alloys are of incredible technological significance, specifically for the ground transport networks. At the point when high quality, great erosion resistance, and high durability are required related to good formability and weldability, aluminium alloys with Mg and Si as alloying components are utilized. The comparison of practical and theoretical outcomes under the multilinear hardening of the aluminium alloys has a significant purpose to pick which material would be good to a specific end.

A few techniques to analyse multilinear hardening have been created over the most recent forty years and basically, because of the changes in the direction and the ratio which is caused due to the principle stress, old methodologies are not generally moderate under multiaxial loads.

Thus, in the most recent decades, a few multilinear hardening methods dependent on a critical plane and furthermore on vital, invariant, and vitality approaches have been proposed. In this paper have used multilinear hardening curves to analyse the cyclic behaviours of the AZ31 alloy.

AZ31 alloy reacts differently for tensile and compression load tests in both monotonic and cyclic loading conditions. Under cyclic loading with stress and strain along vertical axis vis-a-vis equivalent plastic strain on horizontal axis, it is possible to understand the behaviour of the alloy and measure the fatigue failure in the alloy.

During the processing of material under tensile load, deformation in material occurs. There are also possibilities of material failure in tensile loading condition.

In this paper, plasticity of magnesium alloy using multilinear isotropic and multi-linear kinematic hardening properties and the behaviour of the alloy under cycle load condition using Finite Element method are discussed. Finite Element analysis will be carried out with ANSYS software to analyse the results. Finite element method can yield accurate results by reducing manual calculations. Static structural analysis can be done by performing the tensile test, compression, torsional tests, etc., to obtain maximum stress, strain, von-mises, plastic strain, elastic strain, safety factor, and fatigue results. Eight simulations are performed in this paper, two simulations are performed in each of the categories namely multi-linear isotropic hardening, and multi-linear kinematic hardening properties. Moreover, in each of the mentioned categories, two simulations with linear element with mesh size 0.4mm and 0.6mm and two other simulations with quadratic element with mesh size 0.4mm and 0.6mm are performed. In this simulation a cyclic loading is applied to specimen with change in displacement from 0-7.5mm.

## II. LITERATURE REVIEW

### Types of AZ Alloys

J Bholen [1] has explained that AZ alloy is the development of Mg alloys which contains Al and Zn with Al having the highest rate of fixation. The similar compounds that can be obtained from this alloy are AZ31, AZ61, AZ80 and AZ91. The AZ compound is formed from the series of arrangement of aluminium and Zinc by combining their chemical numbers. The AZ alloy in the AZ arrangement is highly preferred in the application of cast and fashioned application which results in great cast ability and possess profound mechanical properties. Al complexion in the AZ alloy enables the development of the  $\beta$ -Mg<sub>17</sub>Al<sub>12</sub> stage and the measurement of the developed compound is influenced from the deformability condition of the surface of development [10]. The author states that high Al compound allows the series of the Al combinations of the Mg<sub>17</sub>Al<sub>12</sub>, and weakens the basal surface by opposing the development of indistinguishable limits and blocking formability. AZ combinations with high Al complexion are, therefore, most favoured for constructional applications.

The formability of these compounds appeared at the closest scale of alloying constituents, particularly increments of different rare elements (RE). [2] revealed that smaller scale alloying increases Ca and Ce in AZ31 alloys resulting in a slight improvement in formability.

Manuscript received on June 09, 2021.

Revised Manuscript received on June 12, 2021.

Manuscript published on June 30, 2021.

\* Correspondence Author

Venkata Sai Prashanth Sudula\*, Graduate Student, Department of Mechanical Engineering, Federation University Australia, Ballarat, Australia. E-mail: [venkatasaiprashanthsudula@gmail.com](mailto:venkatasaiprashanthsudula@gmail.com)

© The Authors. Published by Blue Eyes Intelligence Engineering and Sciences Publication (BEIESP). This is an open access article under the BY-NC-ND license (<http://creativecommons.org/licenses/by-nc-nd/4.0/>)

Grain refinement was observed to scale up with increment in merging alloy combinations which comes in good quality. He also stated that an improvement in rollability and expanded performance of non-basal slip planes and surface changes when AZ31 combinations were adjusted with Li alloying growth. Du, Zheng et al. announced the development of mechanical properties (extreme elasticity, yield quality, and extension) of AZ80 Mg composites with the expansion of Sn (Du et al., 2016). The composites with low convergences of Sn (<2%) have the best mix of properties after heat treatment.

**Cyclic Behaviour of AZ31 alloy**

AZ31 alloys are exceptionally alluring for light-weight developments due to the generally high solidarity to thickness proportions. Till recently, the greater part of the material is utilized for segments like mobile phones, gears, or clutches. Of late, there is an expanding request to utilize the material additionally, for consistently stacked basic parts and if conceivable, at higher assistance temperatures. To show the conduct of complex parts, for example by limited component technique, materials properties must be known. Cyclic lifetimes of the created compound AZ31 and the cast alloy AZ91 at room temperatures up to 300 degrees were researched and characterised. Harm parameters were resolved to portray the cyclic deformation behaviour [3]. The plastic strain amplitudes increase with increase in temperatures and when this happens repetitively cyclic lifetimes reduces. The increased temperature plastic strain amplitudes measure materials destruction during cyclic loading. The deforming behaviour of the two materials namely, AZ 31 and AZ 91 change from cyclic hardening to cyclic softening. As of now, at a temperature of 150 degrees Celsius, cyclic lifetimes of both compounds decreased and contrasted at the room temperature. Under pressure-controlled stacking conditions, cyclic haul was seen at higher temperature. Cyclic behaviour prompts a difference in the deformation affecting the Coffin-Manson connection. Under the mean loading condition at a temperature, the negative mean pressure increases the cyclic lifetime and the positive mean pressure decreases the cyclic lifetime.

[4] has noted that the stress difference between monotonic and cyclic values is about 50 MPa and for the compressive forces, this difference is about 20 MPa. Cyclic loading behaviour of materials along with monotonic behaviour of AZ31 reacts when a load is applied continuously. He further discussed von-misses results with tensile loading conditions and concluded that AZ31 magnesium alloy shows different behaviours under tensile and compression regime. At tension, it was observed that a cyclic hardening behaviour occurs (was verified a cyclic hardening) and at compression state, a slight softening behaviour was observed. From the below Figures1(a) and Figure1(b), [4] discussed 1/2 strain cycle vs. axial strain when there is a change in strain percentage along with the variation of material when a cyclic and monotonic load is applied.

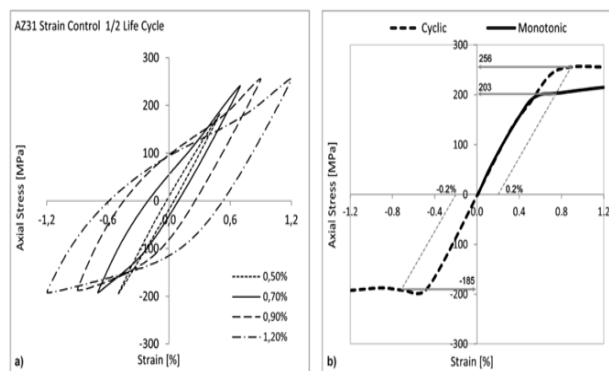


**Figure 1. a & b: Half fatigue life hysteresis loops and b) AZ31 monotonic and cyclic behaviour [4].**

**Yield function**

According to Callister, the stress-strain behaviour of a material is defined as “the degree to which a structure deforms, or strains depend on the magnitude of an imposed stress” [8]. Most metals stressed in tension are relatively at low levels where stress and strain are proportional to each other. This is known as Hooke’s law. Hooke’s law can be used to calculate stress before yielding occurs. According to Matos, yield function is used to begin plastic deformation. This function describes the combinations of stresses that cause material to yield [9]. Matos has given the equation for von-mises criterion in Figure 2.

$$\begin{aligned}
 \text{yield function} &= Y_F \\
 &= \sigma_x^2 + \sigma_y^2 + \sigma_z^2 - \sigma_x \sigma_y - \sigma_y \sigma_z - \sigma_z \sigma_x \\
 &\quad + 3(\tau_{xy}^2 + \tau_{yz}^2 + \tau_{zx}^2) = \sigma_{yield}^2
 \end{aligned}$$

On the other hand [6], stated that plastic behaviour of homogenous isotropic materials is represented by a yield function.

$$F(\sigma_{ij}) = f(\sigma_{ij}) - \sigma_y$$

Where as

$f(\sigma_{ij}) = \sigma_e$  – equivalent stress, depends on stress strain contour

$\sigma_y$  – material yield parameter.

Yield function describes the surface in the stress space that demarks the stress between elastic and plastic behaviour of materials. This is called as yield surface.

There are three possible cases that stress state can occur.

- $F(\sigma_{ij}) < 0$ , the equivalent stress is lower than material yield  $f(\sigma_{ij}) < \sigma_y$ . The stress state at this point is inside the yield surface area with no plastic strain occurrence.
- $F(\sigma_{ij}) = 0$  Plasticity condition equates the equivalent stress with material yield
- $f(\sigma_{ij}) = \sigma_y$ . Stress point lies on the yield surface
- $F(\sigma_{ij}) > 0$ , plastic behaviour of material occurs.

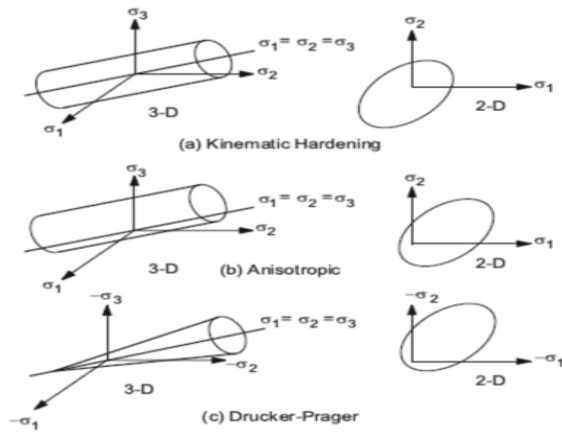


Figure 2. Various yield surfaces [6]

Stresses and strains during material plastic deformation show a dependence on prior loading history. Incremental plasticity model procedure is implemented to identify the dependence through the relation between stress and strain (Matos, 2010). Typical increments of strain are decomposed plastic and elastic strain components.

$$d\varepsilon = d\varepsilon^e + d\varepsilon^p$$

Basan considers it as associative when the plastic potential and yield function are equal ( $Q = F$ ). According to Ducker's theory, this is valid equation for stable materials. Adds Ducker, the yield surface is convex and vector of the plastic strain increment on a smooth point of the yield surface which is directed outward of the normal yield surface [6]. He explained differences between associative flow rule and non-associative flow rule in which the plastic potential is not equal to yield function. The difference between associative flow rule and non-associative flow rule is explained in below.

$$d\varepsilon_{ij}^{pl} = \lambda \frac{\partial Q}{\partial \sigma_{ij}}$$

Where

$\lambda$  = plastic multiplier

$Q$  = function of stress termed the plastic potential

**Material Hardening and Plasticity of the material**

Linear elasticity is a useful parameter in modelling when deformation in the material has high impact over the specimen under load conditions. Almost, most of the engineering materials have slight permanent deformation on removal of the load.

In deformation there are two variants namely reversible and irreversible. In reversible deformation, on load application the strain energy is stored in the material and a form of deformation is observed. Once the load is removed, the strain energy is released, and material regains its original posture. But in irreversible deformation, the energy is not stored in the material, but it is dissipated causing a change in posture of the material.

Permanent deformation is observed in the material when yield stress is above the critical value. Plastic deformation is observed only beyond yield point while load permanent deformation is observed till the crystal structure of the material is disturbed and migration of the grain at micro level is achieved. However, stress induced in the material is independent of the load applied.

In load condition unidirectional case, material will undergo deformation up to yield point Y and then undergoes hardening. Figure 3 depicts uni-axial load stress strain curve.

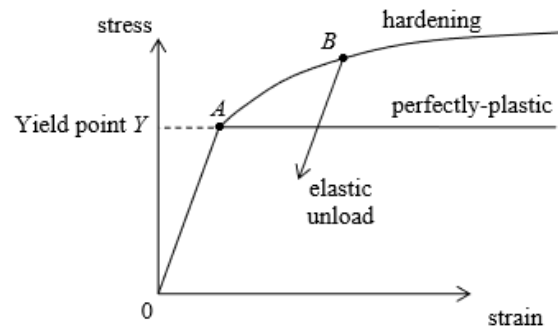


Figure 3. stress strain curve for metal [5]

Once the stress reaches from initial value to point A, specimen is under yield stress. From 0 to point A, the specimen is on elastic load and the material can withstand without any permanent deformation. When the stress moves from point A to point B, slight or negligible deformation that is allowable is observed in the material, and from point B onwards perfect plasticity is gained in the material [5]. Material elastic unloading occurs from point B when the stress is reduced. However, loading must be continued to achieve plastic deformation when the material has to be hardened after yield stress.

Robert Basan's hardening rule represents the condition for establishment of subsequent yielding behaviour after the occurrence of initial yielding. According to him, the point of stress space cannot lie outside the yield surface which has to change its size for further yielding to occur [6]. There are two hardening rules namely, Isotropic hardening rule and Kinematic hardening rule.

In Isotropic hardening, the yield stress is maintained equally in compression and tension load condition while in Kinematic hardening, the elastic range is constant throughout deformation. When a sample is under tension load, Bauschinger effect is observed in the material. Bauschinger effect is the variation in the yield stress between the compression and tension load on the sample. When the specimen reaches maximum yield strength under tension load the sample undergoes compression load. At this point, the yield stress observed at the tension load and compression is different. This effect is clearly illustrated in Figure 4. In the Figure, the real material response is depicted in solid line and the extreme cases in plasticity models are expressed in dotted lines.

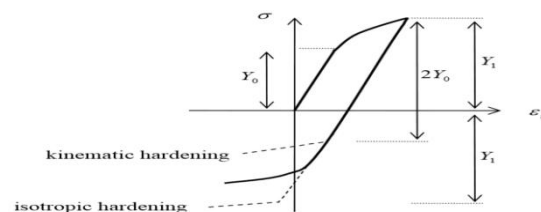
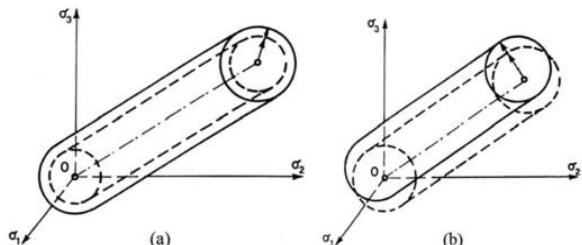


Figure 4. Bauschinger effect [5]



**Isotropic Hardening and Kinematic Hardening**

In Isotropic hardening rule, yield surface remains centered about its center line ( $\sigma_1 = \sigma_2 = \sigma_3$ ) in stress space and expands or shrinks in size as plastic strain develops whereas Kinematic hardening rule presumes that the translation of the yield surface through the stress space with progressive yielding result in the yield surface remaining constant in size, Figure 5.



**Figure 5. Types of hardening (a) isotropic hardening (b) kinematic hardening [6]**

Zhang stated that the hysteresis loops are independent on the strain amplitude for the strain ranges under cyclic hardening tension compression [7]. The author discussed tension-compression and torsional cyclic loading conditions using the cyclic hardening process. He observed that as the number of cycles increase, hardening of material also increases. He also noticed differences at different strain amplitudes of 1%, 0.5%, and 0.2% in figure 6.

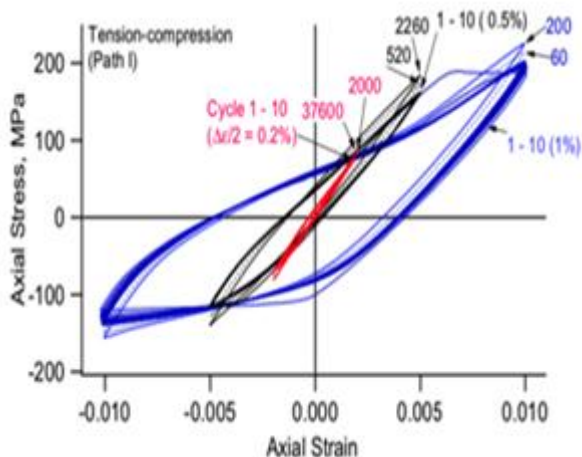


**Figure 6. Stress–strain hysteresis loops under fully reversed strain-controlled tension–compression ( $\Delta\epsilon/2 = 0.2\%$ ,  $0.5\%$ , and  $1.0\%$ ). (Zhang et al., 2011)**

According to [3], the plastic strain amplitude increases with change in time and remains constant until the strain increases over the number of cycles (Figure 6). The plastic strain amplitudes are same in all the events. The plastic strain amplitude decreases with strain and then increases with increasing stress. He discussed monotonic curve and half life cycle of magnesium alloy. He also compared monotonic results with cyclic hardening process to determine cyclic loading behaviour and fatigue life.

**Material and Material Properties**

In this paper, to study plasticity which is one of the properties of AZ31 type magnesium material, cyclic loading behaviour is applied. The chemical composition of

AZ31type magnesium alloy used in this study is given in table 1.

**Table 1. Composition of AZ31 alloy.**

Al	3.1
Zn	1.2
Mn	0.2
Si	0.05
Cu	0.05
Ca	0.04
Fe	0.005
Ni	0.1
Other	0.4
Mg	Balance

The below mentioned material properties were considered for theoretical calculations in table 2 below.

**Table 2. Material properties of AZ31 alloy**

Density	1.77 g/cm <sup>3</sup>
Tensile strength	296MPa
Compressive yield strength	97MPa
Shear strength	130 MPa
Elastic modulus	45GPa
Poisson's ratio	0.32
Elongation at break (50mm)	15%
Bearing yield strength	250MPa

Source: <https://www.azom.com/article.aspx?ArticleID=6707>

Aluminium is the most used material in the aerospace industries and is it used for packing material for food. Also, aluminium is the base material for the versatile paint. High resistance to corrosion is the property that draws automobile attention in selecting material for the interior parts. Low density is the main purpose for using in the structure applications. Strength to weight ratio of the aluminium material is very high and is another reason for selecting material for building the parts for aircraft industries. Cyclic loading is more important parameter for developing parts out of aluminium since the young's modulus is lower and density of the material is low.

**III. METHODOLOGY**

**Multi-Linear (Isotropic, Kinematic) Hardening Curve**

In kinematic hardening the yield surface remains constant in size and translates in the direction of yielding. When a load or displacement applied on specimen after attaining plastic deformation, the specimen will not come to its original position due to behaviour of hardening curve.



In ANSYS finite element method, to perform multi-linear hardening simulation, one must calculate plastic strain and true strain from monotonic tensile test data. As

monotonic tensile test data is huge, consider few points to give as an input in software. Required calculations and data is provided in Figure 7.

Strain	Stress (MPa)	true strain	true stress(Mpa)	elastic strain	plastic strain	true stress (Pa)
0.04	17.83381	0.010220313	18.117882	0.000000000	0.010220313	18117888.2
0.5099347	182.4835	0.409413769	274.7299262	0.006105109	0.403308659	274729926.2
1.0295951	342.1534	0.70603922	400.586871	0.01000193	0.695537289	400586871
1.500285	252.2537	0.917104401	631.1475863	0.014025502	0.903078899	631147586.3
2.014118	258.5256	1.10330725	779.2266644	0.017316148	1.085991102	779226664.4
2.517575	263.7631	1.257771832	927.8064865	0.020617922	1.23715391	927806486.5
3.006238	267.7316	1.387852646	1072.59651	0.023835478	1.364017168	1072596510
3.500813	271.6856	1.504258047	1222.58104	0.027168468	1.47708958	1222581040
4.014389	275.0075	1.612311579	1378.994583	0.030644324	1.581667255	1378994583
4.507014	277.8003	1.706022552	1529.850141	0.03399667	1.672025883	1529850141
5.003154	280.4758	1.792284998	1683.739421	0.037416432	1.754868966	1683739421
5.507136	282.7344	1.872896347	1839.785530	0.040884123	1.832612224	1839785530
6.014359	284.8236	1.947959334	1997.854982	0.044396777	1.902562556	1997854982
6.503798	286.5894	2.015409292	2158.508967	0.047960088	1.967620204	2158508967
7.015133	288.0172	2.08133138	2308.456164	0.051299915	2.030031465	2308456164
7.509191	289.4261	2.140290962	2460.674943	0.0544881665	2.085600296	2460674943
8.021729	290.6919	2.199636001	2622.543544	0.058278745	2.14357255	2622543544
8.510416	291.7303	2.252356074	2774.388094	0.061653089	2.190702985	2774388094
9.003865	292.62	2.302971518	2927.330976	0.065051799	2.237919719	2927330976
9.503224	293.3656	2.351682258	3081.284611	0.068472951	2.28320096	3081284611
10.00429	293.9771	2.398285197	3235.009262	0.071889095	2.326396102	3235009262
10.51133	294.555	2.443331768	3390.719866	0.075349329	2.367982436	3390719866
11.01383	294.9473	2.486889514	3546.396194	0.078868804	2.40808171	3546396194
11.52056	295.34	2.52972093	3697.82219	0.082173826	2.445198267	3697822190
12.0278	295.6432	2.566700132	3850.083329	0.085557407	2.481142724	3850083329
12.45189	295.7344	2.599119617	3978.186618	0.088404147	2.51071547	3978186618
12.90757	295.8246	2.630101843	4130.373523	0.091786078	2.546232353	4130373523

Figure 7. calculation of true stress, elastic strain, and plastic strain.

To input plastic strain and stress in ANSYS initially, true strain and true stress need to be calculated.

$$\text{True strain} = \ln(1 + \text{strain})$$

$$\text{True stress} = \text{stress}(1 + \text{strain})$$

In next step, calculate elastic strain.

$$\text{elastic strain} = (\text{true stress})/E$$

Where E is young's modulus of AZ31 = 45000MPa (45GPa) After calculating elastic strain, plastic strain is calculated by subtracting true strain from elastic strain.

$$\text{Plastic strain} = \text{elastic strain} - \text{true strain}$$

The above-mentioned calculations are considered from ANSYS student support to derive true stress and plastic strain.

<https://studentcommunity.ansys.com/thread/Multi-linear-kinematic-plasticity-material-model-create-from-a-stress-strain-graph/?order=all#comment-e6945286-75dd-4163-b6ca-a81c000d4c7a>(Dated 18/05/2020)

Plastic strain obtained from above calculation is used to input in simulation to determine plastic strain on AZ31 alloy under cyclic loading behaviour. True stress vs plastic strain and stress vs strain have been plotted to show difference between calculated and practical values. To verify calculated values, a logarithmic graph is plotted between true stress vs plastic strain using points after yield stress to plot a linear line. Above calculated plastic strain is used as an input in ANSYS software to calculate plastic strain acting on AZ31 alloy under cyclic loading behaviour.

### Multi-Linear Isotropic Hardening or Multi-Linear Kinematic Hardening Curve

In ANSYS, to obtain multi-linear hardening (isotropic or kinematic) curves, plastic strain and true stress acting upon specimen need to be determined. Results for this simulation are obtained from monotonic tensile test. As test data is huge, few points are considered to give input to software to get accurate results. Stress and strain points are considered for every 0.05mm increase in displacement. The calculations are discussed in mechanical properties in preceding topic.

All inputs to this simulation are in mm and MPa. Plastic strain starts from zero strain and the maximum plastic strain observed is around 2.5mm at true stress around 4500MPa. Multi-linear isotropic and Multi-linear kinematic hardening curve looks similar to each other and the input to these two hardening curves are also the same.

In this simulation a specimen of dimensions 3mm\*20mm (diameter\*length). One end of the specimen is fixed and

other end of specimen a cyclic displacement is applied. From monotonic tensile test huge data few displacement points are considered as input for cyclic loading condition with time as independent variable. Displacement from 1mm to 7.5mm has been given to cyclic loading condition. Strain has been increased from 0 –1mm to 1mm to 0, repeat this procedure from 0-2mm to 2mm-0 and continue same procedure up to 7.5mm to make input as cyclic loading. The displacement is assigned to specimen by cyclic loading, maximum displacement acting as 7.5mm and at final step of this simulation displacement is heading to zero at 466 steps.

## IV. RESULTS

### 4.1 Multi-Linear Isotropic Hardening

#### 4.1.1 Multi-Linear Isotropic Hardening – 0.4mm Linear Mesh

The simulation is about plastic strain when multi-linear isotropic hardening property is assigned to AZ31 specimen. While performing simulation, linear and quadratic element with mesh size 0.4mm and 0.6mm is assigned to the specimen to study cyclic loading behaviour.

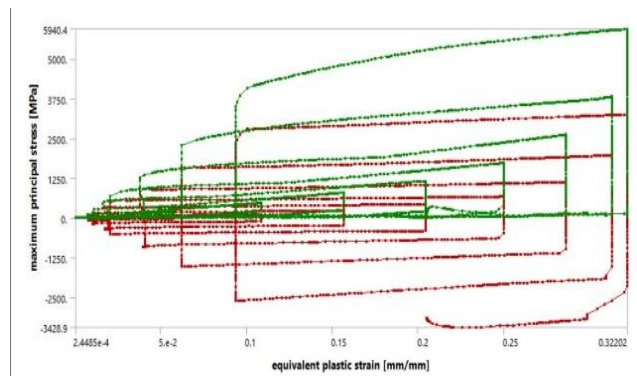


Figure 8. Multi-linear isotropic hardening – 0.4mm linear mesh, Maximum principal stress vs Equivalent plastic strain.



Figure 8 plots maximum principal stress (MPa) vs equivalent plastic strain(mm). The maximum stress observed during last tensile cycle is 5904MPa. The stress difference between 7th cycle and last cycle is almost 2000MPa. In this plot, the stress increase is not linear and keeps on increasing like loops for every cycle. The maximum equivalent plastic strain acting on AZ31 is around 0.32mm during last cycle while in the 7th cycle; the plastic strain is around 0.30mm. The maximum compression stress acting on AZ31 is around -3428MPa by the end of the simulation.

In below Figure 9, the plot is between middle principal stress (MPa) and equivalent plastic strain(mm). The maximum-middle principal stress during last tensile cycle is observed as 4339MPa and maximum-middle principal stress during last compression cycle is noted as -3472MPa. In middle principal stress vs plastic strain plot, we can observe tensile and compression cycles acting on AZ31 clearly whereas in Figure 6 we can observe tensile and compression cycles imposing on each other because of maximum and minimum stress acting on the specimen.

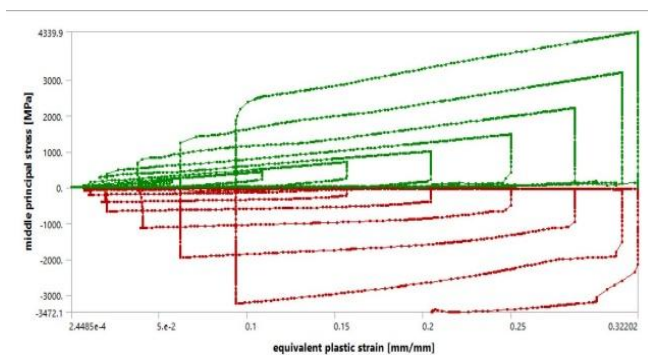


Figure 9. Multi-linear isotropic hardening – 0.4mm linear mesh, Middle principal stress vs Equivalent plastic strain

#### 4.1.2 Multi-Linear Isotropic Hardening – 0.4mm Quadratic Mesh

In Figure 10, the plot is between maximum principal stress (MPa) and equivalent plastic strain(mm) acting on AZ31 during cyclic loading behaviour. The maximum stress acting on the specimen during tensile loading is 7113MPa which is represented using green line. During last three cycles the stress difference between each cycle is around 2000MPa. The red line represents the maximum stress during compression cycle which is around -3200MPa. The equivalent plastic strain during the last compression cycle has become flat and by the end of the simulation it is around 0.21mm.

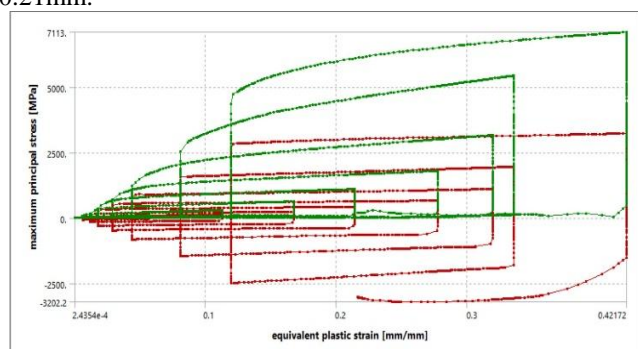


Figure 10. Multi-linear kinematic hardening – 0.4mm quadratic mesh, Maximum principal stress vs Equivalent plastic strain

In below Figure 11, while comparing middle principal stress (MPa) with equivalent plastic strain(mm), the tensile stress during the last cycle is around 3659MPa and the stress during compression cycle is around -3650MPa.

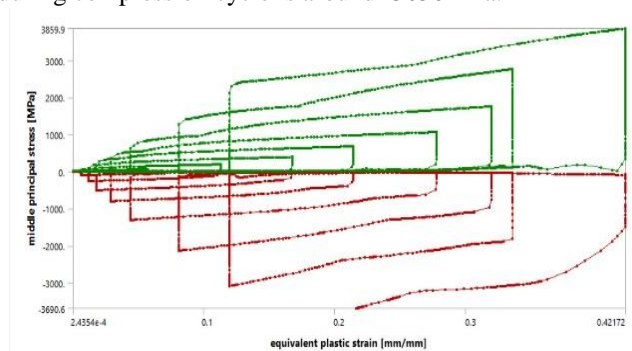


Figure 11. Multi-linear isotropic hardening – 0.4mm quadratic mesh, Middle principal stress vs Equivalent plastic strain

#### 4.1.3 Multi-Linear Isotropic Hardening - 0.6mm Linear Mesh

In below Figure 12, the plot is between maximum principal stress (MPa) and equivalent plastic strain(mm). In the simulation, the maximum stress acting on the specimen during tensile cycle is 5229MPa and during compression cycle, the maximum stress is around -3387MPa by the end of the simulation. The plastic strain acting on AZ31 during the last cycle is 0.3114mm. During compression cycle, the plastic strain has dropped down to 0.20mm and shot up to 0.35mm by the end of the simulation.

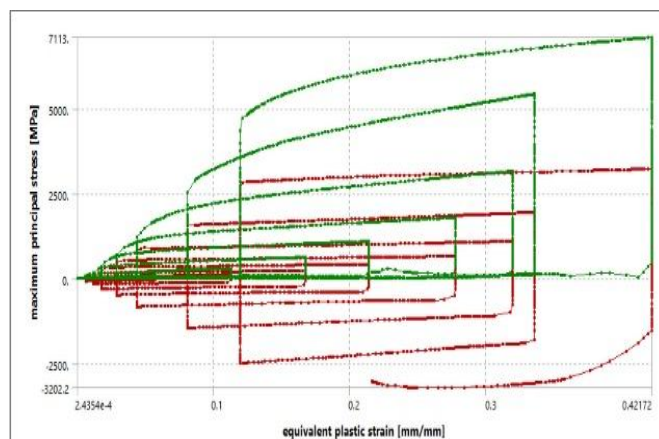
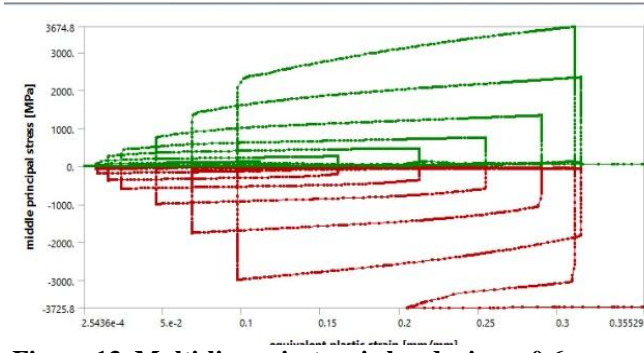


Figure 12. Multi-linear isotropic hardening – 0.6mm linear mesh, Maximum principal stress vs Equivalent plastic strain

The below Figure 13 relates middle principal stress (MPa) with equivalent plastic strain (mm). The maximum-middle principal stress during tensile cycle is 3674.8MPa and maximum-middle principal stress during compression cycle is -3725.8MPa. The middle principal stress during the first 5 tensile and compression cycles is below 1000MPa.



**Figure 13. Multi-linear isotropic hardening – 0.6mm linear mesh, Middle principal stress vs Equivalent plastic strain**

**4.1.4 Multi-Linear Isotropic Hardening – 0.6mm Quadratic Mesh**

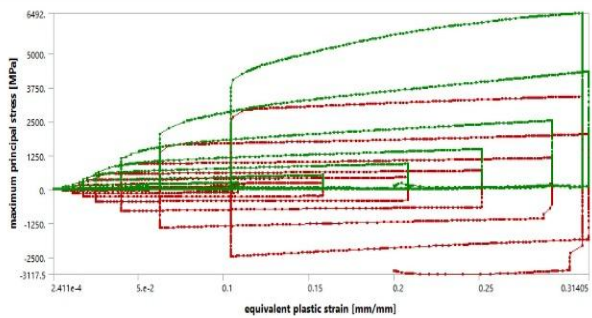


**Figure 14. Multi-linear isotropic hardening – 0.6mm quadratic mesh, Maximum principal stress vs Equivalent plastic strain**

The above Figure 14 explains maximum principal stress acting on AZ31 during cyclic loading behaviour with displacement as an input to this simulation. The maximum principal stress acting on specimen during tensile cycle is around 6492MPa. The stress difference between last three cycles is around 1500MPa. The maximum equivalent plastic strain acting on the specimen is 0.31mm during 8th cycle and the strain at the end of the simulation is 0.20mm. Maximum stress acting on AZ31 specimen during compression cycle is around -3117MPa. The stress during first 5 tensile and compression cycles is less than 1000MPa. In Figure 15, the maximum-middle principal stress acting on specimen during the last cycle is 3142MPa and the stress during 7th cycle is around 2000MPa with a stress difference of around 1200MPa. The maximum-middle principal stress acting during compression cycle is -3144MPa with plastic strain less than the 7th cycle.

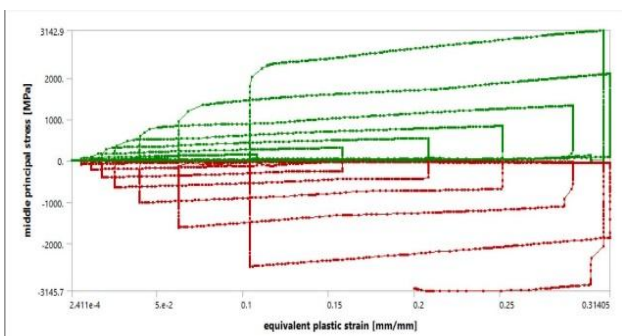


**Figure 15. Multi-linear isotropic hardening – 0.6mm linear mesh, Middle principal stress vs Equivalent plastic strain**

**4.2 Multi-Linear Kinematic Hardening**

In this simulation the variable parameters are mesh size 0.4mm and 0.6mm with linear and quadratic element type. The input for the simulation is cyclic displacement up to 7.5mm. The plot is between equivalent stress and equivalent plastic strain.

**4.2.1 Multi-Linear Kinematic Hardening - 0.4mm Linear Mesh**

The below Figure16 explains plot between equivalent stress (MPa) and equivalent plastic strain(mm). The equivalent stress acting on AZ31 during the last cycle is 277.72MPa. The increase in stress per cycle is around 40MPa. In this simulation, the stress for every cycle is following linear path in continuation of pervious cycle showing that specimen is holding energy and displacement. The maximum plastic strain at the end of the simulation is 0.40mm.

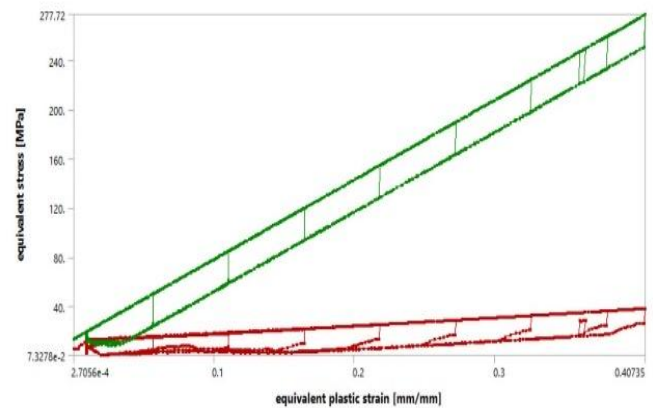


**Figure 16. Multi-linear kinematic hardening – 0.4mm linear mesh, Equivalent stress vs equivalent plastic strain**

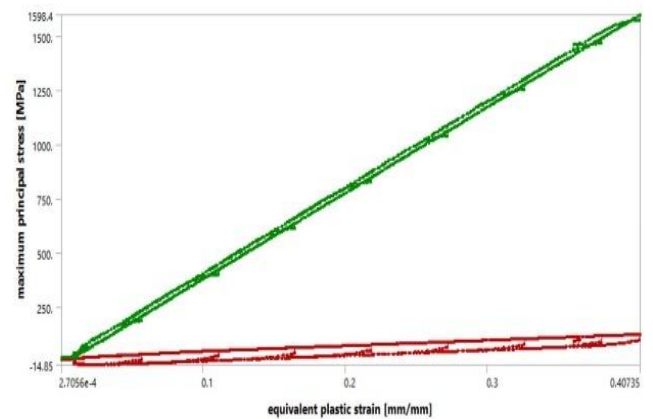


**Figure 17. Multi-linear kinematic hardening – 0.4mm linear mesh, Maximum principal stress vs Equivalent plastic strain.**

The above Figure 17 explains plot between maximum principal stress (MPa) and equivalent plastic strain (mm). The maximum stress acting on AZ31 during the last cycle is around 1598MPa. The compression cycle can be observed with minimal stress acting on specimen.



Middle principal stress acting on AZ31 during tensile cycle with maximum stress at around 1520MPa. The stress increase in between cycles beginning with the initial cycle is 250MPa. The equivalent plastic strain acting on AZ31 specimen is 0.407mm. The increase in plastic strain gets reduced in the last three cycles showing maximum plasticity of specimen.

**4.2.2 Multi-Linear Kinematic Hardening - 0.4mm Quadratic Mesh**

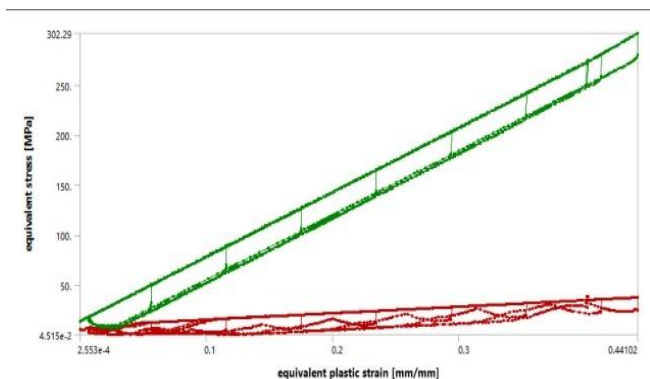


**Figure 18. Multi-linear kinematic hardening – 0.4mm quadratic mesh, Equivalent stress vs equivalent plastic strain**

The above Figure 18 plots equivalent stress (MPa) vs equivalent plastic strain(mm). The equivalent stress acting on the specimen is around 302MPa during the last tensile cycle. The maximum plastic strain during the last cycle is around 0.44mm. The increase in stress per cycle is around 50MPa per cycle.

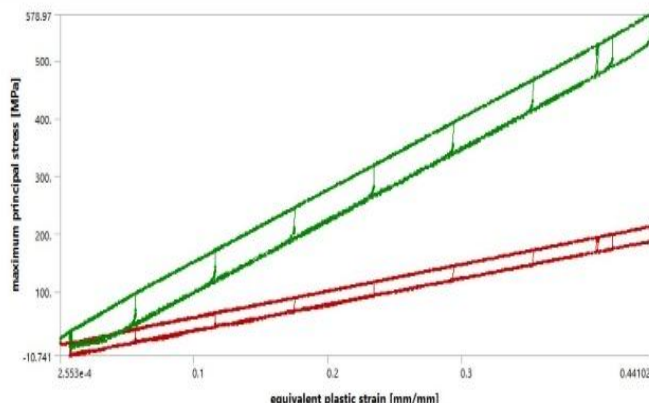


**Figure 19. Multi-linear kinematic hardening – 0.4mm quadratic mesh, Maximum principal stress vs Equivalent plastic strain**

The above plot in Figure 19 is to relate maximum principal stress (MPa) with equivalent plastic strain(mm). The maximum stress observed during this simulation is around 578MPa and the maximum equivalent strain observed during the last cycle is about 0.44mm. Middle principal stress (MPa) and equivalent plastic strain(mm). The maximum-middle principal stress acting on AZ31 is 378MPa. The average increase in stress per cycle is around 60MPa.

**4.2.3 Multi-Linear Kinematic Hardening – 0.6mm Linear Mesh**

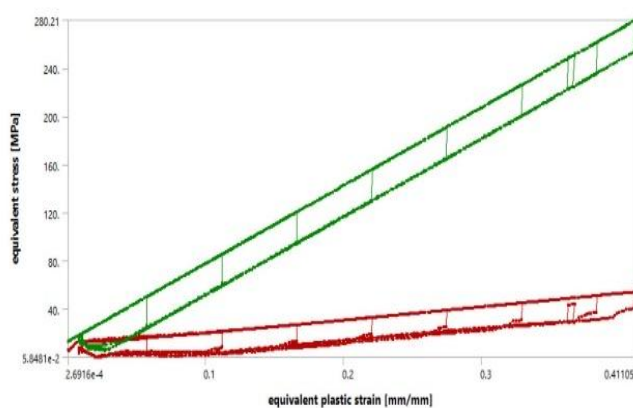


**Figure 20. Multi-linear kinematic hardening – 0.4mm linear mesh, Equivalent stress vs Equivalent plastic strain**

The above plot 20 is between equivalent stress (MPa) and equivalent plastic strain (mm). The maximum stress acting on specimen during cyclic loading observed is around 280.1MPa. The plot is linear showing specimen holding stress from cycle to cycle after the application of cyclic load. The equivalent plastic strain acting on the specimen is 0.411mm during the last cycle.

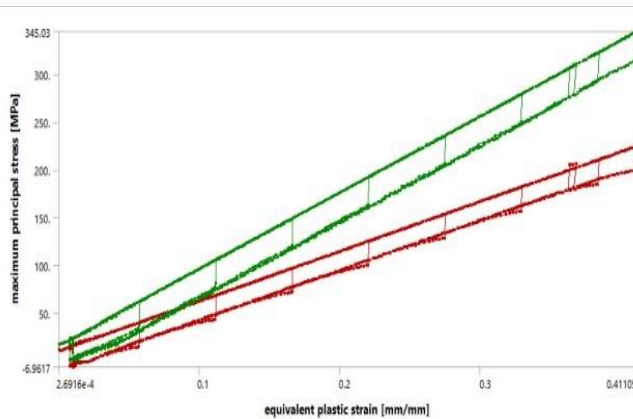


**Figure 21. Multi-linear kinematic hardening – 0.4mm linear mesh, Maximum principal stress vs Equivalent plastic strain**

The figure 21 explains about maximum principal stress (MPa) vs equivalent plastic strain(mm) acting on AZ31. It is observed that the maximum principal stress acting on specimen is around 345.03MPa and the equivalent plastic strain at the end of the simulation is around 0.410mm. The maximum-medium principal stress during tensile cycle on AZ31 is 232MPa. The stress acting on specimen during the second cycle is around 80MPa with strain 0.11mm. In this simulation, AZ31 specimen will store energy or displacement after every cycle that leads to lower stress values when compared with multi-linear isotropic hardening curve results.



4.2.4 Multi-Linear Kinematic Hardening – 0.6mm Quadratic Mesh

The Figure 22 explains equivalent stress (MPa) vs equivalent plastic strain (mm) acting on AZ31 specimen. The maximum stress observed during this simulation is 278.4MPa. The equivalent plastic strain observed during the last cycle by the end of the simulation is 0.403mm.

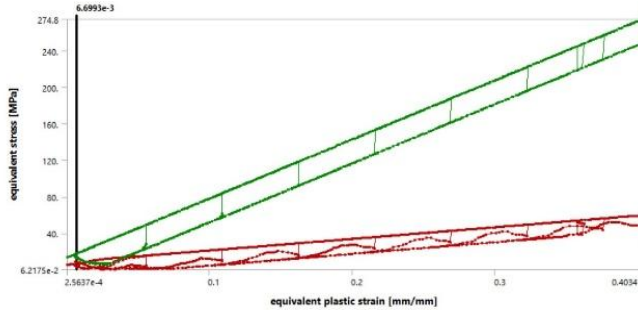


Figure 22. Multi-linear kinematic hardening – 0.6mm quadratic mesh equivalent stress vs Equivalent plastic Strain

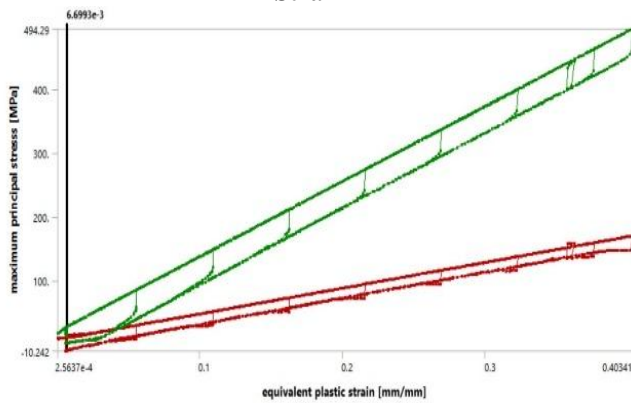


Figure 23. Multi-linear kinematic hardening – 0.6mm quadratic mesh, Maximum principal stress vs Equivalent plastic strain.

The above Figure 23 explains plot between maximum principal stress (MPa) and equivalent plastic strain (mm). The maximum stress observed during the last cycle is 494MPa. The average increase in stress per cycle for the first 6 cycles is around 70MPa and during the last two cycles a minor change in stress is observed. The middle principal stress is 308MPa at the end of the simulation.

V. DISCUSSIONS AND CONCLUSIONS



Figure 24. linear and quadratic element type with 0.4mm and 0.6mm mesh size, multi-linear isotropic hardening

The above Figure 24 explains plot between linear and quadratic element type with 0.4mm and 0.6mm mesh size when cyclic displacement is acting on AZ31. In this simulation, plastic strain at the end of the simulation did not reach zero but stopped at a point during compression cycle. The maximum equivalent plastic strain during 2nd cycle is 0.1130mm in simulation with quadratic element 0.4mm mesh size, the minimum equivalent plastic strain observed in both linear and quadratic element type 0.4mm and 0.6mm linear mesh as 0.108mm. Maximum plasticity noticed during 4th cycle with quadratic element 0.4mm mesh size is 0.212mm and with linear mesh 0.6mm the plasticity is 0.212mm. The maximum plastic strain during the 6th cycle is 0.319mm with quadratic element 0.6mm mesh by the end of the simulation. During 7th cycle, the plastic strain observed is 0.3356mm and during the last cycle it shot up to 0.421mm. At the end of the simulation permanent strain acting on specimen is around 0.216mm, the minimum plasticity in linear element 0.4mm mesh during 4th cycle is 0.204mm, during 6th cycle is 0.2863mm and 0.3131mm during 7th cycle. At the end of the simulation plasticity is 0.2049mm for linear element 0.6mm mesh. Maximum plasticity noticed is 0.3555mm and with minimum value of 0.20 mm for quadratic element 0.6mm mesh. The minimum plasticity during last cycle observed is 0.31mm.

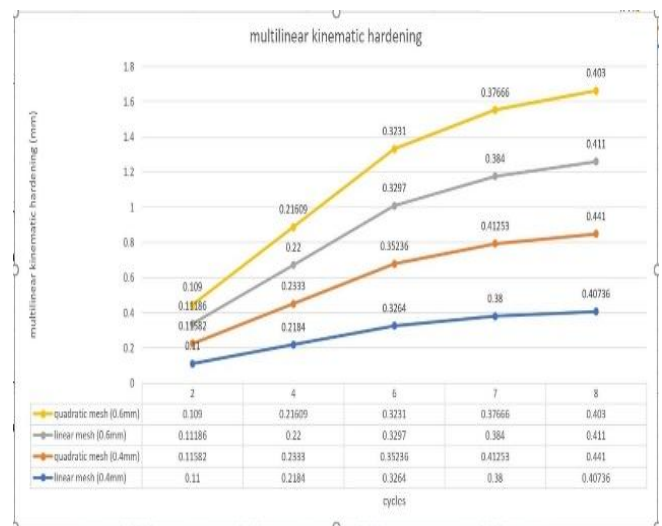


Figure 25. Explains plasticity acting on AZ31 during cyclicloading using multi-linear kinematic hardening

The above Figure 25 explains plasticity acting on AZ31 during cyclic loading using multi-linear kinematic hardening property with linear and quadratic element 0.4mm and 0.6mm mesh. In this Figure, plastic strain from 2nd cycle to last cycle is observed wherein maximum plastic strain observed on specimen during 2nd cycle is 0.115mm in quadratic element 0.4mm mesh. The minimum plasticity can be noticed in quadratic element 0.6mm mesh as 0.109mm. During 4th cycle, minimum plasticity with a strain of 0.316mm is observed in two simulations with linear element 0.4mm mesh and quadratic element 0.6mm mesh.



Maximum plasticity during 6th cycle under quadratic element 0.4mm mesh is 0.3523mm, and minimum plasticity during 6th cycle is 0.323mm with quadratic element 0.6mm mesh. The maximum plastic strain can be observed till the end of the simulation in quadratic element 0.4mm mesh. The strain observed during 7th cycle 0.41253mm and during 8th cycle the strain is 0.441mm. The lowest plastic strain at the end of the last cycle is 0.403mm for quadratic element linear mesh simulation. From above two Figures, maximum plasticity can be noticed in quadratic element 0.4mm linear meshing multi-linear isotropic hardening simulation and the maximum plasticity acting on AZ31 is 0.421mm and 0.441mm for multi-linear kinematic hardening simulation. In all the 16 simulations conducted till the end of the experiment, the maximum plastic strain 0.4425mm is observed in bilinear kinematic hardening 0.4mm mesh with linear element. On arriving to the conclusion of this paper, the objective of the project is achieved which help of the technological assistants. Comparing the isotropic and kinematic hardening for the magnesium alloy with linear and quadratic mesh was carried out successful. The future scope of this project would help in the application of magnesium alloy in aviation and the other automobile manufacturing. The future scope of work, we have noticed cyclic hysteresis loops for multilinear isotropic hardening curve whereas for multi-linear kinematic hardening curve have observed overlapped loops in the positive quadrant. Change in displacement both positive and negative may result to have better results

### REFERENCES

1. Stutz, L., Bohlen, J., Letzig, D., & Kainer, K. U. (2011). Formability of magnesium sheet ZE10 and AZ31 with respect to initial texture. In *Magnesium Technology 2011* (pp. 373-378): Springer.
2. Masoumi, M., & Pegguleryuz, M. (2011). The influence of Sr on the microstructure and texture evolution of rolled Mg-1% Zn alloy. *Materials Science and Engineering: A*, 529, 207-214.
3. Albinmousa, J., Jahed, H., & Lambert, S. (2011). Cyclic axial and cyclic torsional behaviour of extruded AZ31B magnesium alloy. *International Journal of Fatigue*, 33(11), 1403-1416.
4. Anes, V., Reis, L., Li, B. L., & Freitas, M. *Multiaxial Fatigue Behaviour (HCF and LCF) of AZ31 Magnesium Alloy*.
5. Kelly, P. (2013). *Solid Mechanics. Part II, Lecture notes, The University of Auckland*.
6. (Robert Basan, 2016) [http://www.riteh.uniri.hr/media/filer\\_public/c7/b4/c7b4b975-9474-4b66-a04f-ff3597ba61e7/d711\\_constitutive\\_modeling\\_and\\_material\\_behavior\\_int\\_erm\\_report.pdf](http://www.riteh.uniri.hr/media/filer_public/c7/b4/c7b4b975-9474-4b66-a04f-ff3597ba61e7/d711_constitutive_modeling_and_material_behavior_int_erm_report.pdf) (06/09/2020)
7. Zhang, J., Yu, Q., Jiang, Y., & Li, Q. (2011). An experimental study of cyclic deformation of extruded AZ61A magnesium alloy. *International Journal of Plasticity*, 27(5), 768-787.
8. Callister, W. D., & Rethwisch, D. G. (2007). *Materials science and engineering: an introduction* (Vol. 7): John Wiley & Sons New York.
9. Matos, A. (2010). *Multiaxial Fatigue Simulation of an AZ31 Magnesium Alloy using ANSYS and a Plasticity Program*.
10. Stutz, L., Bohlen, J., Letzig, D., & Kainer, K. U. (2011). Formability of magnesium sheet ZE10 and AZ31 with respect to initial texture. In *Magnesium Technology 2011* (pp. 373-378): Springer.

### AUTHORS PROFILE



**Venkata Sai Prashanth Sudula**, pursued master's in mechanical engineering at Federation University - Australia. Pursuing MBA- Aviation Management and PGP - Logistics and supply chain management. Design and Development of micro controller drone for civil application, Thermo -Structural analysis in expansion joints on liner and non-liner bellow and bilinear isotropic and bilinear kinematic hardening of AZ31 Magnesium Alloy. Engineers Australia - E grad member.